Diagn Interv Radiol 2025; DOI: 10.4274/dir.2026.263687

HYBRID IMAGING AND NUCLEAR MEDICINE

ORIGINAL ARTICLE

Microvascular dysfunction in patients with transthyretin cardiac amyloidosis evaluated by 13N-ammonia positron emission tomography–computed tomography: is it an early marker of the disease?

Aristóteles Neto[1]
Caio Cafezeiro[1]
Bruno Bueno[1]
Cristhian Espinoza Romero[1]
Vitor Emer Rosa[1]
Viviane Hotta[1]
Camila de Godoi Carneiro[2]
Carlos Rochitte[1]
Vagner Madrini[1]
Jose Soares[1]
William Chalela[1]
Marcos Lima[2]
Carlos Buchpiguel[2]
Edward Miller[3]
Fabio Fernandes[1]

[1]Heart Institute (InCor), Hospital das Clínicas HCFMUSP, Faculdade de Medicina, Universidade de São Paulo, São Paulo, Brazil

[2]Department of Radiology, Hospital das Clínicas da Faculdade de Medicina da Universidade de São Paulo (HCFMUSP), São Paulo, Brazil

[3]Medicine and Radiology in the Section of Cardiovascular Medicine in Yale New Heaven Hospital, Connecticut, United States

PURPOSE

To evaluate coronary microvascular function using 13N-ammonia positron emission tomography/computed tomography in individuals with pathogenic *transthyretin* (TTR) gene mutations, with and without cardiac involvement. This study is the first to assess coronary flow reserve (CFR) in this population before overt cardiac amyloidosis (CA) is detectable by conventional imaging.

METHODS

We evaluated microvascular impairment by measuring CFR in 20 patients with and 20 patients without cardiac involvement due to TTR amyloidosis (ATTR), all presumed to be free from epicardial coronary artery disease and carrying *TTR* gene mutations.

RESULTS

The study revealed a significantly reduced mean global CFR in the cardiac involvement group (1.849 ± 0.379 vs. 2.952 ± 0.7, $P < 0.001$). Global CFR inversely correlated with age, functional class, troponin, and B-type natriuretic peptide while positively correlating with the 6-minute walk test distance, mean blood pressure, and global longitudinal strain. Receiver operating characteristic curve analysis identified an optimal cutoff value of global CFR < 2.58, yielding a sensitivity of 100% and a specificity of 75% for detecting cardiac involvement.

CONCLUSION

In patients with ATTR CA, coronary microvascular dysfunction emerges as a clinically relevant marker of cardiac involvement, even in the absence of structural abnormalities or obstructive coronary disease.

CLINICAL SIGNIFICANCE

CFR assessment may aid in diagnostic suspicion, risk stratification, and understanding of angina symptoms in this population.

KEYWORDS

Amyloidosis, microvascular blood flow, coronary arteries

Corresponding author: Cristhian Espinoza Romero

E-mail: cristhian.153@hotmail.com

Received 08 October 2025; revision requested 22 December 2025; accepted 14 January 2026.

Epub: 04.02.2026

Publication date:

DOI: 10.4274/dir.2026.263687

Transthyretin (TTR) amyloidosis (ATTR) affects the heart through the deposition of amyloid fibrils. Early biomarkers, such as troponins, often indicate damage to cardiomyocytes and the coronary microvasculature.[1,2] ATTR occurs either in a hereditary form, caused by *TTR* gene mutations, or in a wild-type form, typically associated with aging. In both entities, positron emission tomography/computed tomography (PET/CT) has emerged as a valuable tool for assessing microvascular dysfunction, enabling early evaluation of myocardial perfusion and coronary flow reserve (CFR) impairment in this population.[2-5] Cardiac amyloidosis (CA) compromises the microvasculature via fibril-induced thickening, extrinsic vessel

You may cite this article as: Neto A, Cafezeiro C, Bueno B, et al. Microvascular dysfunction in patients with transthyretin cardiac amyloidosis evaluated by 13N-ammonia positron emission tomography–computed tomography: is it an early marker of the disease? *Diagn Interv Radiol*. 04 February 2026 DOI: 10.4274/dir.2026.263687 [Epub Ahead of Print].

compression, or endothelial and autonomic dysfunction.[1] Patients with CA frequently exhibit chronic troponin elevation, electrically inactive regions on the electrocardiogram, and anginal symptoms, and signs of ischemia have been reported in some individuals with CA without obstructive epicardial coronary artery disease (CAD).[2-5]

Given the scarcity of studies evaluating coronary microvascular dysfunction in ATTR, this is the first known study to employ 13N-ammonia PET/CT to assess CFR in individuals exclusively carrying TTR mutations without evident cardiac involvement on standard imaging examinations. However, a previous study evaluated 31 patients with CA, including 15 with light-chain amyloidosis (AL) and 6 with ATTR, and compared them with patients with left ventricular hypertrophy secondary to hypertension. In that study, microvascular dysfunction was more prevalent in patients with CA-ATTR.[6-9] Another study evaluated 400 patients with CA-ATTR; however, microvascular obstruction, assessed using magnetic resonance imaging, was present in 221 (27.6%) patients and was more common in CA-ATTR than in CA with AL.[5]

The primary aim of this research is to assess microvascular function in individuals with pathogenic *TTR* gene mutations, both with and without cardiac involvement. Using 13N-ammonia PET/CT, we evaluated CFR and its correlation with clinical, laboratory, and imaging variables.

Methods

Study design and population

A total of 40 individuals carrying pathogenic *TTR* gene mutations were prospectively enrolled (Supplementary Figure 1). Participants were divided into two groups:

- Group A (n = 20): patients with evidence of cardiac involvement
- Group B (n = 20): patients without cardiac involvement.

Main points

- Patients with cardiac involvement exhibit significantly reduced coronary flow reserve (CFR).
- Coronary microvascular dysfunction emerges as a clinically relevant marker of cardiac involvement.
- CFR assessment may aid in diagnostic suspicion, risk stratification, and understanding of angina symptoms in this population.

Additionally, as part of the initial protocol focused on cardiac elastography, another group of 20 patients was included as healthy controls; CFR was not assessed in these individuals. First-degree relatives of patients with hereditary ATTR who elected to undergo genetic testing after genetic counseling were included. Those testing positive for an ATTR-compatible mutation were referred from external services to the cardiomyopathy specialist institutions participating in the study.

Inclusion criteria

- Age ≥18 years
- Confirmed pathogenic mutation in the *TTR* gene
- Ability to provide informed consent

Cardiac involvement, defined by the presence of at least one of the following:

- Interventricular septal thickness > 12 mm on echocardiography or cardiac magnetic resonance imaging, in the absence of other causes of hypertrophy (e.g., hypertension and aortic stenosis)
- History of heart failure symptoms or signs consistent with CA
- Elevated cardiac biomarkers [troponin or B-type natriuretic peptide (BNP)] without an alternative explanation
- Positive Congo red staining in tissue biopsy or Grade 2 or 3 cardiac uptake on 99mTc-pyrophosphate scintigraphy, with monoclonal gammopathy of undetermined significance ruled out

The exclusion criteria are provided in the Supplementary appendix. Wild-type TTR CA was excluded.

PET/CT imaging protocol: Coronary microvascular blood flow (MBF) was assessed using dynamic 13N-ammonia PET/CT imaging at rest and during pharmacologic stress induced by intravenous dipyridamole. MBF quantification was performed using time–activity curves derived from the blood pool and myocardium, corrected for partial volume effects and spill-over.

CFR calculation: This was calculated as the ratio of stress MBF to rest MBF, according to the 17-segment model proposed by the American Society of Nuclear Cardiology.[10,11] Rest MBF values were normalized using the rate–pressure product to account for individual variations in cardiac workload.

All 40 patients included in the study underwent calcium score assessment as a screening measure to minimize bias related to CAD, which was low in both groups (Supplementary Table 1). The cut-off values used were 40 ng/L for troponin and 35 pg/mL for BNP. This study was approved by the Ethics Committee of InCor (CAAE 27437019.5.0000.0068) through a substantiated opinion on February 6, 2020. All participants provided written informed consent prior to inclusion, under the supervision and approval of the institutional ethics committee.

Statistical analysis

The sample size was determined pragmatically based on patient availability. Continuous variables are reported as mean ± standard deviation when normally distributed and as median (interquartile range) or median ± median absolute deviation when distributional assumptions were violated. The t-test was used to compare means between two groups when both normality (Shapiro–Wilk) and homoscedasticity (Levene) assumptions were met. When either assumption was violated, the Mann–Whitney U test was applied. The null hypothesis (H_0) for all comparisons stated that no significant difference existed between groups. Where H_0 was rejected, effect size was calculated using Cohen's d (d: 0.2–0.5 = small, 0.5–0.8 = moderate, > 0.8 = large).

Pearson's correlation coefficient (r) was used to quantify linear relationships between parametric variables. Spearman's rank correlation coefficient (ρ) was applied for non-parametric variables. Both coefficients range from −1 to +1, with values approaching either extreme indicating stronger associations. For performance analysis, receiver operating characteristic curve analysis and the Youden index were used to establish the optimal cutoff point. A multivariable regression model was constructed, including covariates such as age, blood pressure, sex, a non-zero coronary artery calcium score, and biomarkers.

All statistical tests were two-tailed, and $P < 0.05$ was considered statistically significant. Analyses were performed using JASP software, version 0.16.3 JASP software, version 0.16.3 (JASP Team, Amsterdam, The Netherlands).[12]

Results

Baseline characteristics

The main clinical and structural characteristics of the study population are summa-

rized in Table 1. The remaining characteristics are summarized in Supplementary Tables 1, 2, 3 and 4.

Differences between the groups were evident. Patients with cardiac involvement exhibited conditions consistent with longer exposure to amyloid deposition: they were older and had a higher body mass index, greater interventricular septal thickness, atrial enlargement, lower left ventricular ejection fraction, lower left ventricular global longitudinal strain (LVGLS) and right ventricular global longitudinal strain (RVGLS), more advanced degrees of diastolic dysfunction, poorer functional capacity, and worse performance on the 6-minute walk test, with a shorter total distance. In addition, they had higher cardiac biomarker levels, including troponin and BNP. This group also showed a higher prevalence of chronic conditions such as hypertension and diabetes. Despite the diagnosis of hypertension, patients reported not using antihypertensive medications and had normal or reduced blood pressure levels at the time of consultation. No patient with type 2 diabetes mellitus required insulin for glycemic control. There was no history of anginal symptoms, coronary atherosclerotic disease, or use of anti-ischemic medications or prior revascularization in either group. In the groups with pathological variants of the *TTR* gene, the most prevalent mutations were Val142Ile, followed by Val50Met and Thr80Ala, with no statistically significant differences in mutation type between the groups.

Global coronary flow reserve

Mean global CFR was significantly lower in the cardiac involvement group (1.849 ± 0.379) than in the non-involvement group (2.952 ± 0.7; $P < 0.001$) (Figure 1, Table 2). Global CFR showed an inverse correlation with age, functional class according to the New York Heart Association classification, troponin, and BNP levels, and it showed a positive correlation with total distance in the 6-minute walk test and mean arterial pressure. Accordingly, older age, higher functional class according to the NYHA classification, and elevated serum troponin and BNP levels were associated with worse global CFR. Conversely, better performance on the walk test was associated with higher global CFR (Figure 2, Table 3, Supplementary Table 5).

CFR also correlated with multiple clinical, laboratory, and echocardiographic parameters, including markers of left and right ventricular systolic and diastolic function, as well as indices of structural remodeling in both ventricles and atria (Table 3). Notably, global CFR demonstrated significant associations with predictors of subclinical myocardial involvement, such as LVGLS and RVGLS (Figure 2).

Segmental CFR analysis revealed lower values in the CA group, particularly in apical segments. This reduction was evident both when segments were grouped according to epicardial artery territories and when analyzed individually (Table 4).

Receiver operating characteristic curve analyses

Receiver operating characteristic curve analysis identified a global CFR cut-off of < 2.58 to differentiate cardiac involvement, with a sensitivity of 100% and specificity of 75%, an area under the curve of 0.902 (0.80–1.0), and a *P* value of <0.001 (Supplementary Figure 2). In Supplementary Figure 3 we can see the genetic profile of the patients included in the study.

Coronary flow reserve and ischemic disease equivalent

In the cardiac involvement group, 60% (n = 12) demonstrated a global CFR consistent with ischemic disease (≤ 2.5), whereas only 15% (n = 3) of the non-involvement group exhibited similar findings.

Discussion

The main findings of this study support the inclusion of anginal symptoms in the absence of obstructive epicardial CAD as a relevant clinical feature when suspecting CA in patients with TTR mutations. Additionally, our results emphasize the potential role of coronary microvascular dysfunction as a pathophysiological marker of the disease, revealing a global perfusion impairment pattern that resembles three-vessel CAD, including the apical region.

This study further advances the concept of coronary microvascular dysfunction as a hallmark of CA, a prototypical extracellular storage disorder characterized by insoluble fibril deposition, a hypertrophic phenotype, and extensive structural remodeling.[2-5]

The coexistence of microvascular dysfunction and structural abnormalities in the setting of restrictive cardiomyopathy underscores the need for comprehensive functional assessments.[4-7] Our findings highlight a potential dissociation between structural and functional impairment, as evidenced by patients with reduced CFR but lacking con-

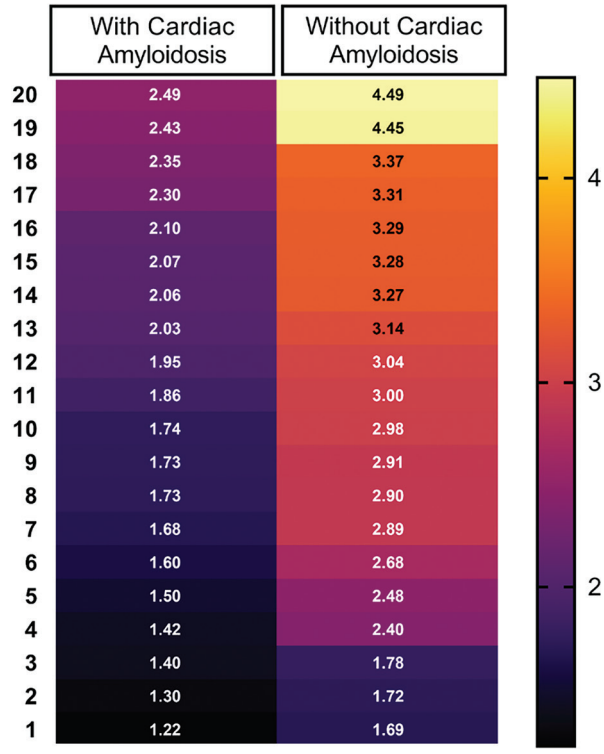

Figure 1. Heat map: global coronary flow reserve (CFR). Heat map representing global CFR distribution across study groups: each column corresponds to a study group, and each row represents an individual patient. Color intensity reflects CFR values, with lighter shades indicating higher (better) CFR and darker shades indicating lower (worse) CFR. This visualization highlights differences in microvascular function between groups.

ventional markers of cardiac involvement. Among patients with established cardiac involvement, 60% exhibited a global CFR pattern consistent with ischemic heart disease, whereas only 15% of those without cardiac involvement showed similar findings. These results are consistent with previously reported CFR thresholds for epicardial CAD.[13]

In contrast to prior studies, our data demonstrate that CFR impairment may occur independently of anginal symptoms.[1,14] Notably, 15% of patients without overt cardiac involvement based on standard diagnostic criteria had CFR values indicative of ischemic disease, suggesting the presence of subclinical microvascular dysfunction.

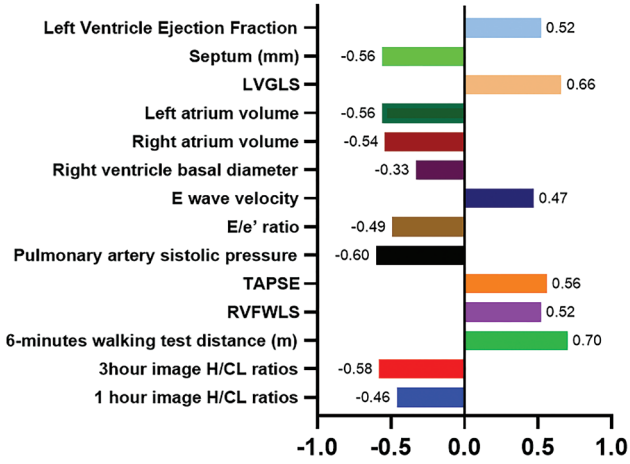

Figure 2. Didactic representation of significant correlations of global coronary flow reserve. Bars represent the strength and direction of correlations, with positive and negative associations indicated accordingly. Numerical values next to each bar denote the correlation coefficients, reflecting the magnitude of the relationships between variables. LVGLS, left ventricular global longitudinal strain; TAPSE, tricuspid annular plane systolic excursion; RVFWLS, right ventricular free wall longitudinal strain; H/CL, heart-to-contralateral ratio.

Table 1. Baseline clinical and laboratory characteristics of patients

Variable	ATTR with CA (n = 20)	ATTR without CA (n = 20)	*P* value
Demographics			
Age (years)	69.6 ± 8.2	41.6 ± 10.8	< 0.001
Male sex	16 (80.0)	11 (55.0)	0.177
Arterial hypertension	12 (60.0)	5 (25.0)	< 0.001
Diabetes mellitus	9 (45.0)	3 (15.0)	< 0.001
BMI (kg/m^2)	23.85 ± 3.0	25.8 ± 4.7	0.146
Hemodynamics			
Heart rate (bpm)	74.4 ± 10.5	69.9 ± 9.5	0.17
SBP (mmHg)	117.9 ± 21.3	128.0 ± 17.9	0.12
MBP (mmHg)	89.5 ± 14.4	94.3 ± 25.1	0.45
Clinical features			
Carpal tunnel syndrome (%)	13 (65)	3 (15)	0.005
Extracardiac involvement (%)	14 (70)	7 (35)	0.027
6-minute walk test distance (m)	336.9 ± 83.7	420.4 ± 112.8	< 0.001
Chest pain (%)	4 (20)	2 (10)	0.66
Functional class (NYHA)			
Class I (%)	4 (20)	20 (100)	-
Class II (%)	14 (70)	0 (0)	-
Class III (%)	2 (10)	0 (0)	-
Biomarkers			
Troponin (ng/L)	63.7 ± 41.2	7.15 ± 10.7	< 0.001
BNP (pg/mL)	389.5 (210–545)	14 (12.5–24)	< 0.001

ATTR, transthyretin amyloidosis; CA, cardiac amyloidosis; BMI, body mass index; bpm, beats per minute; SBP, systolic blood pressure; MBP, mean blood pressure; NYHA, New York Heart Association classification; BNP, B-type natriuretic peptide.

A novel and clinically relevant observation was the absence of apical microvascular preservation in the cardiac involvement group, despite preserved apical longitudinal strain on speckle-tracking echocardiography. This is the first study to report such a discrepancy, highlighting a unique pattern of microvascular involvement that can be effectively detected using 13N-ammonia PET/CT imaging.

Koyama and Falk[15] demonstrated that reduced longitudinal deformation is associated with poorer survival in patients with AL. However, our findings, derived exclusively from a population with CA-ATTR, suggest that coronary microvascular dysfunction driven by a higher amyloid burden may represent the mechanistic link underlying impaired longitudinal deformation.

Importantly, early-stage amyloidosis without overt myocardial infiltration may still present with anginal symptoms due to microvascular obstruction, which has been associated with worse prognosis in this condition.[16] A prevalence of up to 3% has been reported among patients with amyloidosis and angiographically normal coronary arteries.[3] Although the exact frequency of amyloid-related angina remains unclear, the presence of chest pain in patients with suspected amyloidosis warrants careful evaluation.

Finally, our study validated a CFR cut-off value of 2.58, which demonstrated high sensitivity and specificity for detecting cardiac involvement. These findings suggest that early functional assessments, such as CFR evaluation, may complement structural imaging modalities in identifying early cardiac amyloid infiltration.

This study is limited by its small sample size and the lack of invasive coronary artery assessment due to ethical and safety considerations. However, the use of calcium scoring and the diffuse CFR reduction pattern provided reliable insights into microvascular function. Further studies are warranted to validate these findings in larger cohorts. Another limitation is the small and uneven sample, with a significant age disparity between groups (patients without cardiac involvement in hereditary ATTR are typically identified at a young age). Furthermore, the study sample was selected using conveni-

Table 2. Coronary flow reserve in patients with and without cardiac involvement

Coronary territory	ATTR with cardiac involvement (n = 20)	ATTR without cardiac involvement (n = 19)	*P* value	Cohen's d
Global CFR	1.849 ± 0.379	2.952 ± 0.700	<0.001	1.878
Left anterior descending	1.886 ± 0.364	2.970 ± 0.787	<0.001	1.767
Left circumflex	1.911 ± 0.437	3.087 ± 0.873	<0.001	1.704
Right coronary artery	1.886 (1.63–2.13)	2.900 ± 0.804	<0.001	−0.600

Values are reported as mean ± standard deviation, n/N (%), or median (25^{th}–75^{th} percentile), as appropriate. ATTR, transthyretin amyloidosis; CFR, coronary flow reserve.

Table 3. Global CFR clinical correlations

Correlation	r	*P* value
Age	−0.701	< 0.001
Weight (kg)	0.174	0.309
Height (m)	0.309	0.067
BMI	0.049	0.785
Heart rate (bpm)	−0.285	0.079
SBP (mmHg)	0.149	0.367
MBP (mmHg)	0.344	0.030
Functional class (NYHA)	−0.553	< 0.001
6-minute walk test distance (m)	0.696	< 0.001
Troponin (ng/L)	−0.581	< 0.001
BNP (pg/mL)	−0.734	< 0.001

BMI, body mass index; SBP, systolic blood pressure; MBP, mean blood pressure; bpm, beats per minute; BNP, B-type natriuretic peptide; NYHA, New York Heart Association classification.

Table 4. Comparison of CFR across the 17 cardiac segments in patients with and without cardiac amyloidosis

		ATTR with AC (n = 20)	ATTR without AC (n = 19)	*P* value	Cohen's d
PET/CT 13N-ammonia					
Basal	Anterior	2.202 ± 0.58	2.802 ± 0.844	0.006	0.843
	Anterolateral	2.213 ± 0.831	3.031 ± 0.981	0.004	0.899
	Inferolateral	1.91 ± 0.501	3.047 ± 0.933	< 0.001	1.518
	Inferior	2.231 ± 1.737	3.133 ± 0.975	0.025	0.641
	Inferoseptal	2.317 ± 1.6	2.714 ± 0.785	< 0.001	0.57
	Anteroseptal	1.959 ± 0.69	2.844 ± 0.696	< 0.001	1.273
Medium	Anterior	1.956 ± 0.409	2.984 ± 0.909	< 0.001	0.730
	Anterolateral	2.071 ± 0.708	3.113 ± 0.962	< 0.001	1.2
	Inferolateral	1.837 ± 0.390	3.26 ± 0.946	< 0.001	1.99
	Inferior	1.929 ± 0.719	3.155 ± 0.95	< 0.001	1.456
	Inferoseptal	2.172 ± 1.652	3.091 ± 0.881	< 0.001	0.755
	Anteroseptal	1.862 ± 0.4	3.061 ± 0.768	< 0.001	1.953
Apical	Anterior	2.0 ± 0.698	2.885 ± 0.71	< 0.001	0.72
	Lateral	2.313 ± 1.89	3.01 ± 0.708	< 0.001	0.765
	Inferior	2.067 ± 1.699	3.012 ± 0.755	< 0.001	0.66
	Septal	1.965 ± 0.69	2.964 ± 0.824	< 0.001	0.7
	Apex	1.603 ± 0.411	3.029 ± 0.741	< 0.001	0.89

ATTR, transthyretin amyloidosis; CA, cardiac amyloidosis; PET/CT, positron emission tomography/computed tomography.

ence sampling, which has the potential to introduce bias. An additional limitation was the use of dipyridamole as the stress agent. Agents such as adenosine or regadenoson have a faster onset of action and more predictable kinetics than dipyridamole; these properties may be more advantageous for the evaluation of absolute myocardial blood flow using PET perfusion tracers. However, dipyridamole is the most widely used, validated, and familiar agent at our institution and, when administered using an appropriate protocol as in the present study, minimizes the probability of errors.

In conclusion, coronary microvascular dysfunction, assessed by 13N-ammonia PET/CT, is a hallmark of CA, with a global involvement pattern mimicking three-vessel CAD. In patients with CA-ATTR, coronary microvascular dysfunction emerges as a clinically relevant marker of cardiac involvement, even in the absence of structural abnormalities or obstructive coronary disease. CFR assessment may aid in diagnostic suspicion, risk stratification, and the understanding of anginal symptoms in this population.

Footnotes

Conflict of interest disclosure

This work was supported financially by Pfizer sponsorship. No other potential conflict of interest relevant to this article was reported.

Supplementary Figures link: https://d2v96fxpocvxx.cloudfront.net/cf9d60d6-523c-458aa2e6-78728d3ffbb0/content-images/2ad30fbc-8742-4fc5-9a13-95775e744b1d.pdf

Supplementary Tables link: https://d2v96fxpocvxx.cloudfront.net/8a9ff4da-541a-42fa9980-1a9a3ab6d6c5/content-images/5deef236fd57-4004-a700-8b7b49126a21.pdf

References

1. Ruberg FL, Grogan M, Hanna M, Kelly JW, Maurer MS. Transthyretin amyloid cardiomyopathy: JACC State-of-the-Art Review. *J Am Coll Cardiol*. 2019;73(22):2872-2891. [Crossref]
2. Ogawa H, Mizuno Y, Ohkawara S, et al. Cardiac amyloidosis presenting as microvascular angina--a case report. *Angiology*. 2001;52(4):273-278. [Crossref]
3. Al Suwaidi J, Velianou JL, Gertz MA, et al. Systemic amyloidosis presenting with angina pectoris. *Ann Intern Med*. 1999;131(11):838-841. [Crossref]
4. Whitaker DC, Tungekar MF, Dussek JE. Angina with a normal coronary angiogram caused by amyloidosis. *Heart*. 2004;90(9):e54. [Crossref]

5. Netti L, Ioannou A, Martinez-Naharro A, et al. Microvascular obstruction in cardiac amyloidosis. *Eur J Heart Fail*. 2025;27(12):2948-2951. [Crossref]
6. Dorbala S, Vangala D, Bruyere J Jr, et al. Coronary microvascular dysfunction is related to abnormalities in myocardial structure and function in cardiac amyloidosis. *JACC Heart Fail*. 2014;2(4):358-367. [Crossref]
7. Rahman JE, Helou EF, Gelzer-Bell R, et al. Noninvasive diagnosis of biopsy-proven cardiac amyloidosis. *J Am Coll Cardiol*. 2004;43(3):410-415. [Crossref]
8. Falk RH, Alexander KM, Liao R, Dorbala S. AL (Light-Chain) Cardiac Amyloidosis: a review of diagnosis and therapy. *J Am Coll Cardiol*. 2016;68(12):1323-1341. [Crossref]
9. Gertz MA, Benson MD, Dyck PJ, et al. Diagnosis, prognosis, and therapy of transthyretin amyloidosis. *J Am Coll Cardiol*. 2015;66(21):2451-2466. [Crossref]
10. Cerqueira MD, Weissman NJ, Dilsizian V, et al. Standardized myocardial segmentation and nomenclature for tomographic imaging of the heart. A statement for healthcare professionals from the Cardiac Imaging Committee of the Council on Clinical Cardiology of the American Heart Association. *Circulation*. 2002;105(4):539-542. [Crossref]
11. Dilsizian V, Bacharach SL, Beanlands RS, et al. ASNC imaging guidelines/SNMMI procedure standard for positron emission tomography (PET) nuclear cardiology procedures. *J Nucl Cardiol*. 2016;23(5):1187-1226. [Crossref]
12. Goss-Sampson M. Statistical Analysis in JASP - A Students Guide v0.10.2. [Internet]. figshare; 2019. [Crossref]
13. Herzog BA, Husmann L, Valenta I, et al. Long-term prognostic value of 13N-ammonia myocardial perfusion positron emission tomography added value of coronary flow reserve. *J Am Coll Cardiol*. 2009;54(2):150-156. [Crossref]
14. Fiechter M, Ghadri JR, Gebhard C, et al. Diagnostic value of 13N-ammonia myocardial perfusion PET: added value of myocardial flow reserve. *J Nucl Med*. 2012;53(8):1230-1234. [Crossref]
15. Koyama J, Falk RH. Prognostic significance of strain Doppler imaging in light-chain amyloidosis. *JACC Cardiovasc Imaging*. 2010;3(4):333-342. [Crossref]
16. Mueller PS, Edwards WD, Gertz MA. Symptomatic ischemic heart disease resulting from obstructive intramural coronary amyloidosis. *Am J Med*. 2000;109(3):181-188. [Crossref]